AD-A050 754 SYRACUSE UNIV N Y DEPT OF ELECTRICAL ENGINEERING F/G 20/3
CIRCUMFERENTIAL DISTRIBUTION OF SCATTERING CURRENT AND SMALL HO--ETC(U)
DEC 77 H K SCHUMAN F30602-75-C-0121

UNCLASSIFIED RADC-TR-77-412 NL

| OF |
AD
A050754

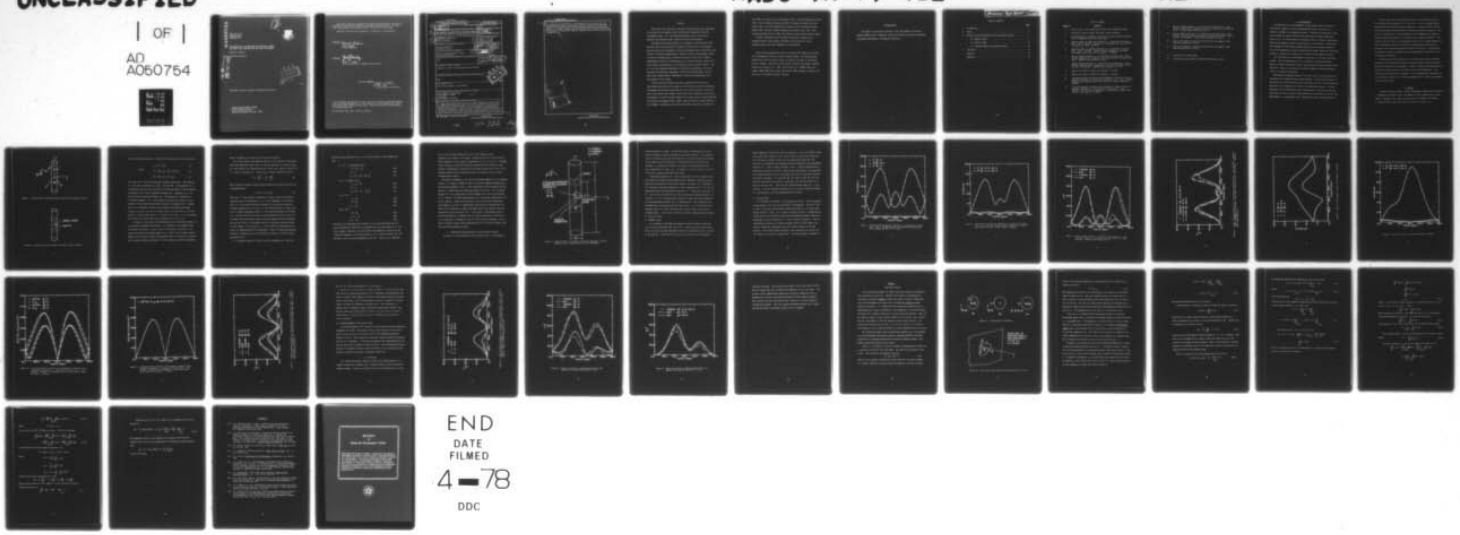

END
DATE
FILMED
4-78
DDC

RADC-TR-77-412
Phase Report
December 1977

CIRCUMFERENTIAL DISTRIBUTION OF SCATTERING CURRENT AND SMALL HOLE COUPLING FOR THIN FINITE CYLINDERS

Harvey K. Schuman

Syracuse University

Approved for public release; distribution unlimited.

ROME AIR DEVELOPMENT CENTER
Air Force Systems Command
Griffiss Air Force Base, New York 13441

This report has been reviewed by the RADC Information Office (OI) and is releasable to the National Technical Information Service (NTIS). At NTIS it will be releasable to the general public, including foreign nations.

RADC-TR-77-412 has been reviewed and is approved for publication.

APPROVED: Jacob Scherer
JACOB SCHERER
Project Engineer

APPROVED: Joseph J. Naresky
JOSEPH J. NARESKY
Chief, Reliability & Compatibility Division

FOR THE COMMANDER: John P. Huss
JOHN P. HUSS
Acting Chief, Plans Office

If your address has changed or if you wish to be removed from the RADC mailing list, or if the addressee is no longer employed by your organization, please notify RADC (RBC) Griffiss AFB NY 13441. This will assist us in maintaining a current mailing list.

Do not return this copy. Retain or destroy.

UNCLASSIFIED

SECURITY CLASSIFICATION OF THIS PAGE (When Data Entered)

REPORT DOCUMENTATION PAGE

READ INSTRUCTIONS BEFORE COMPLETING FORM

1. REPORT NUMBER: RADC-TR-77-412	2. GOVT ACCESSION NO.
3. RECIPIENT'S CATALOG NUMBER	
4. TITLE (and Subtitle): CIRCUMFERENTIAL DISTRIBUTION OF SCATTERING CURRENT AND SMALL HOLE COUPLING FOR THIN FINITE CYLINDERS.	5. TYPE OF REPORT & PERIOD COVERED: Phase Report.
	6. PERFORMING ORG. REPORT NUMBER: N/A
7. AUTHOR(s): Harvey K. Schuman	8. CONTRACT OR GRANT NUMBER(s): F30602-75-C-0121
9. PERFORMING ORGANIZATION NAME AND ADDRESS: Syracuse University, Syracuse NY 13210	10. PROGRAM ELEMENT, PROJECT, TASK AREA & WORK UNIT NUMBERS: 95670016 00
11. CONTROLLING OFFICE NAME AND ADDRESS: Rome Air Development Center (RBC), Griffiss AFB NY 13441	12. REPORT DATE: Dec 77; NUMBER OF PAGES: 33
14. MONITORING AGENCY NAME & ADDRESS (if different from Controlling Office): Same	15. SECURITY CLASS. (of this report): UNCLASSIFIED; 15a. DECLASSIFICATION/DOWNGRADING SCHEDULE: N/A

16. DISTRIBUTION STATEMENT (of this Report)

Approved for public release; distribution unlimited.

17. DISTRIBUTION STATEMENT (of the abstract entered in Block 20, if different from Report)

Same

18. SUPPLEMENTARY NOTES

RADC Project Engineer: Jacob Scherer

19. KEY WORDS (Continue on reverse side if necessary and identify by block number)

Electromagnetic Compatibility
Electromagnetic Fields
Scattering
Electromagnetic Coupling

'theta'

20. ABSTRACT (Continue on reverse side if necessary and identify by block number)

The scattering current induced on a thin, finite, conducting cylinder immersed in a "θ" polarized E-field is studied. Particular attention is paid to the circumferentially non-uniform mode. This non-uniformity is shown significant (peak-to-average ratio of 3 dB at cylinder mid-length) for wavelength long cylinders with diameters as small as 0.067λ. Also investigated is the relationship between scattering current and cavity response patterns for narrow, thin-walled cylindrical cavities with small holes through whcih energy is coupled.

next page

DD FORM 1 JAN 73 1473 EDITION OF 1 NOV 65 IS OBSOLETE

UNCLASSIFIED

SECURITY CLASSIFICATION OF THIS PAGE (When Data Entered)

lambda

339 712

It is demonstrated theoretically, with experimental verification, that the circumferential variation of scattering current strongly affects the fields within thin cylindrical cavities having apertures with small circumferential extents. It is noted, however, that for most thin-body radiation and scattering problems (in contrast with aperture coupling) only the uniform current mode is significant.

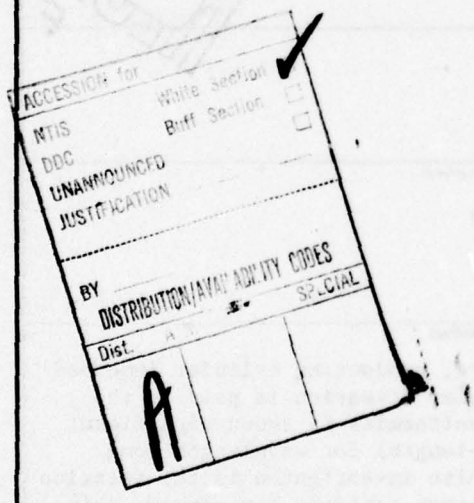

PREFACE

This effort was conducted by Syracuse University under the sponsorship of the Rome Air Development Center Post-Doctoral Program for Rome Air Development Center. Mr. Jack Edwards RADC/RBCA was the task project engineer and provided overall technical direction and guidance.

The RADC Post-Doctoral Program is a cooperative venture between RADC and some sixty-five universities eligible to participate in the program. Syracuse University (Department of Electrical Engineering), Purdue University (School of Electrical Engineering), Georgia Institute of Technology (School of Electrical Engineering), and State University of New York at Buffalo (Department of Electrical Engineering) act as prime contractor schools with other schools participating via sub-contracts with the prime schools. The U.S. Air Force Academy (Department of Electrical Engineering), Air Force Institute of Technology (Department of Electrical Engineering), and the Naval Post Graduate School (Department of Electrical Engineering) also participate in the program.

The Post-Doctoral Program provides an opportunity for faculty at participating universities to spend up to one year full time on exploratory development and problem-solving efforts with the post-doctorals splitting their time between the customer location and their educational institutions. The program is totally customer-funded with current projects being undertaken for Rome Air Development Center (RADC), Space and Missile Systems Organization (SAMSO), Aeronautical System Division (ASD), Electronics Systems Divi-

sion (ESD), Air Force Avionics Laboratory (AFAL), Foreign Technology Division (FTD), Air Force Weapons Laboratory (AFWL), Armament Development and Test Center (ADTC), Air Force Communications Service (AFCS), Aerospace Defense Command (ADC), HQ USAF, Defense Communications Agency (DCA), Navy, Army, Aerospace Medical Division (AMD), and Federal Aviation Administration (FAA).

Further information about the RADC Post-Doctoral Program can be obtained from Mr. Jacob Scherer, RADC/RBC, Griffiss AFB, NY, 13441, telephone Autovon 587-2543, Commercial (315) 330-2543.

This work was performed as part of a larger effort aimed at analyzing the electromagnetic effect of missile exhaust plumes. The participating organizations for the overall effort are Georgia Institute of Technology, Atlanta, Georgia; University of Mississippi, Oxford, Mississippi; Syracuse University, Syracuse, N.Y.; RADC, Griffiss AFB, N.Y.; MICOM, Huntsville, Alabama; OMEW, WSMR, White Sands, New Mexico; NSWC, Dahlgren, Virginia; and University of Colorado, Boulder, Colorado.

ACKNOWLEDGMENT

The author is particularly grateful to Mr. Ron Prehoda of the Naval Surface Weapons Center, Dahlgren, Virginia for helpful discussions regarding experiments performed at the Dahlgren laboratory.

TABLE OF CONTENTS

LIST OF FIGURES

1. Introduction

The penetration of electromagnetic fields through small apertures in rotationally symmetric cavities (approximating cables, missiles, etc.) presents a problem of considerable interest. Theoretical predictions of the cavity fields are usually obtained with variations of "Bethe" Small-Hole Theory [3-6]. In these methods an equivalent cavity excitation, comprised of electric and magnetic dipoles lying adjacent to the aperture, is determined. The strengths of these dipoles depend primarily on the aperture shape and also on the apertureless (replace aperture with perfect conductor) scattering current, $\underset{\sim}{J}$, induced on the body at the location of the shorted aperture.

For thin bodies the circumferential variation of $\underset{\sim}{J}$ is often considered uniform. The non-uniform mode of $\underset{\sim}{J}$ is essentially sinusoidal and thus appears as equal and opposite closely spaced currents which contribute little radiation. Hence, for scatterer and antenna problems a uniform representation of $\underset{\sim}{J}$ is usually sufficient.

With aperture coupling, however, the cavity field is quite sensitive to the portion of $\underset{\sim}{J}$ induced on the shorted aperture. The non-uniform mode of $\underset{\sim}{J}$, significant for even electrically very thin bodies [9, 10], is then important especially if the aperture is limited in circumferential extent. A recent experiment [6] has demonstrated that consideration of only the uniform mode could lend to errors in cavity field prediction on the order of 3 dB for thin, approximately 1.3 wavelengths long cylinders with small circular apertures.

In this report these experimental results are verified theoretically for cylinders with diameters of 0.1λ and 0.067λ . This is accomplished by comparing the experimentally derived "patterns" of detected cavity voltage with theoretically derived patterns of equivalent aperture excitation. The latter is formed from a linear combination of the components of $\underset{\sim}{J}$ and the surface charge (divergence of $\underset{\sim}{J}$) evaluated at the aperture (shorted). The patterns are with respect to the angular direction of an incident plane wave. These comparisons also serve to evaluate a computational method used to determine $\underset{\sim}{J}$ for (otherwise arbitrary) bodies of revolution. In particular the method's accuracy in predicting the circumferential variation of $\underset{\sim}{J}$ for thin bodies is assessed.

The theory is briefly discussed in the next section with a detailed derivation of the relationship between aperture-shorted scattering current and cavity field left to an appendix. Section 3 follows with comparisons of theoretically and experimentally derived cavity-field "patterns". Only incident field polarization orthogonal to the circumferential variation (ϕ) is considered. Hence, the ϕ-directed component of $\underset{\sim}{J}$ is found to contribute little to the results.

2. Theory

Consider the thin, finite, closed, conducting cylinder shown in Figure 1. A coordinate system with z-axis coincident with the cylinder axis is also shown. Throughout this report the excitation is assumed to be $\underset{\sim}{E}^i=\hat{\theta}$V/m, a θ-polarized unit plane wave incident in the $\phi = 0$ plane. The

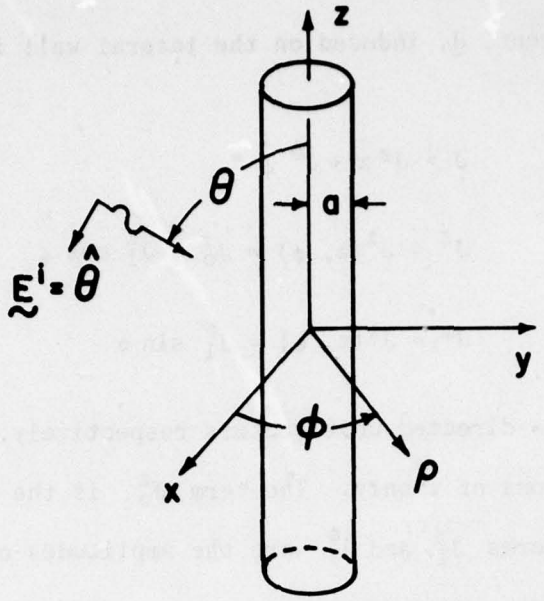

Figure 1. Finite, thin, closed conducting cylinder and coordinate system.

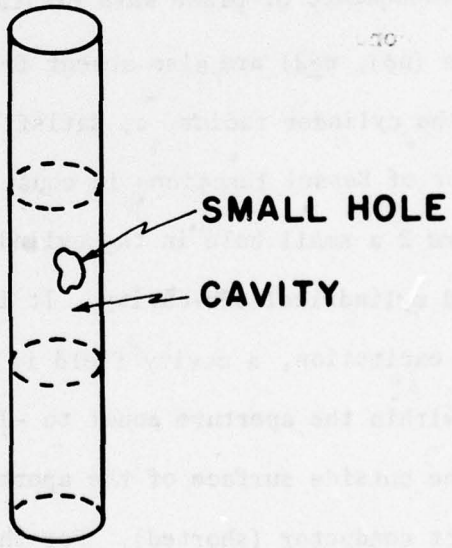

Figure 2. Sub-cavity within cylinder with small lateral aperture.

surface scattering current, $\underset{\sim}{J}$, induced on the lateral wall is then given by

$$\underset{\sim}{J} = J^z \hat{z} + J^\phi \hat{\phi} \tag{1}$$

where

$$J^z = J^z(z, \phi) = J_o^z + J_1^z \cos \phi \tag{2}$$

$$J^\phi = J^\phi(z, \phi) = J_1^\phi \sin \phi \tag{3}$$

and $\hat{z}$ and $\hat{\phi}$ are z- and ϕ-directed unit vectors respectively. The terms J_o^z, J_1^z and J_1^ϕ are functions of z only. The term J_o^z is the uniform -in- ϕ contribution, and the terms J_1^z and J_1^ϕ are the amplitudes of the sinusoidal variations of the z and ϕ components respectively. Equations (2, 3) are given by Body of Revolution Theory [1]. The absence of a uniform-in- ϕ ϕ-directed component, J_o^ϕ, and additional $\cos \phi$ and $\sin \phi$ terms is a consequence of the chosen polarization and plane of incidence of $\underset{\sim}{E}^i$. Furthermore, as a consequence of plane wave excitation the higher order modes ($\sin(n\phi)$, $\cos(n\phi)$, $n \geq 2$) are also absent from (2,3) since they are not significant if the cylinder radius, a, satisfies $2\pi a < \lambda$ where λ is the wavelength (Note behavior of Bessel functions in equations (77, 78) of [2].).

In Figure 2 a small hole in the cylinder wall is shown which connects to a thin-walled cylindrical sub-cavity. It is derived in the Appendix that, for external excitation, a cavity field is equivalently excited by a current source within the aperture equal to $-\underset{\sim}{J}$. Here $\underset{\sim}{J}$ is the surface current induced on the outside surface of the aperture after the aperture is covered with a perfect conductor (shorted). For the external excitation considered

here $\underset{\sim}{J}$ is given by (1) localized to the shorted aperture.

It is also proven in the Appendix that for a flat aperture sufficiently small the significant three terms in a Taylor expansion of $\underset{\sim}{J}$ about a point $\underset{\sim}{P}$ in the aperture, for exciting the cavity field, are linearly related to J^z, J^ϕ , and $\nabla\cdot\underset{\sim}{J}$ evaluated at P. Here $\nabla\cdot\underset{\sim}{J}$ is a surface divergence given by

$$\nabla\cdot\underset{\sim}{J} = \frac{\partial J^z}{\partial z} + \frac{1}{a}\frac{\partial J^\phi}{\partial z} \tag{4}$$

Thus a detected voltage at some location within the cylindrical cavity can be approximated by

$$v = A\hat{J}^z + A' J^\phi + B\hat{\nabla\cdot J} \tag{5}$$

where the "$\hat{}$" sign indicates "evaluation at point $\underset{\sim}{P}$ within the aperture (shorted)" and the coefficients, A, A' , B are independent of excitation. The A, A' , B are usually functions primarily of the aperture shape and internal properties of the cavity. In the simplified case of a small aperture in a plane conducting screen it is well-known from Small Hole Theory [3, 4, 5] that the first two terms on the right-hand side of (5) are contributions from (equivalent) aperture-parallel magnetic dipole components and the last term is a contribution from an (equivalent) aperture-normal electric dipole. In this work A, A', B are treated as normalization constants in comparing theory with experiment. Hence, the only approximation necessary in applying (5) to the structure of Figure 2 is that the small aperture be flat.

It is apparent from (1-4) that $\nabla\cdot\underset{\sim}{J}$ and the components of $\underset{\sim}{J}$ have the

following forms along the $\phi=0$, π, $\pi/2$, and $3\pi/2$ paths on the cylinder surface:

a) $\phi=0$ (Illuminated side) -

$$J^z = J_o^z + J_1^z \tag{6a}$$

$$J^\phi = 0 \tag{6b}$$

$$\nabla\cdot\underset{\sim}{J} = \dot{J}_o^z + \dot{J}_1^z + \frac{1}{a} J_1^\phi \tag{6c}$$

b) $\phi = \pi$ (Shadow side) -

$$J^z = J_o - J_1^z \tag{7a}$$

$$J^\phi = 0 \tag{7b}$$

$$\nabla\cdot\underset{\sim}{J} = \dot{J}_o^z - \dot{J}_1^z - \frac{1}{a} J_1^\phi \tag{7c}$$

c) $\phi = \pi/2$ -

$$J^z = J_o^z \tag{8a}$$

$$J^\phi = J_1^\phi \tag{8b}$$

$$\nabla\cdot\underset{\sim}{J} = \dot{J}_o^z \tag{8c}$$

d) $\phi = 3\pi/2$ -

$$J^z = J_o^z \tag{9a}$$

$$J^\phi = - J_1^\phi \tag{9b}$$

$$\nabla\cdot\underset{\sim}{J} = \dot{J}_o^z \tag{9c}$$

Of course, all right-hand-side variables in (6-9) are functions only of z and all derivatives, denoted by an overhead dot, are with respect to z. For thin cylinders, therefore, the non-uniform circumferential variation of the z-directed component of scattering current, J^z, is characterized by (6a, 7a), and that of the ϕ-directed component by (8b, 9b). Thus, by (5), equations

(6a, 7a, 8b, 9b) also exhibit the cavity field "magnetic mode" dependence on cylinder "roll" angle. Similarly the cavity field "electric mode" dependence on roll angle is governed by (5, 6c, 7c, 8c, 9c). Although fields externally scattered from thin cylinders are not sensitive to non-uniform circumferential variations of scattering current this is not true of aperture coupled fields, particularly when the apertures have only small circumferential extents.

The means of computing $\underset{\sim}{J}$, for the thin cylinder examples in the following section, is a method of moments, body of revolution computer program [1,2]. The governing equation is an $\underset{\sim}{E}$ - field formulation which constrains the tangential $\underset{\sim}{E}$ - field along the conducting surface to be zero. As will become apparent J^{ϕ} is not significant in these examples due to the θ-polarization of $\underset{\sim}{E}^{i}$. However, for other polarizations of $\underset{\sim}{E}^{i}$ an accurate computation of J^{ϕ} may be required. Since, for thin bodies, use of the $\underset{\sim}{E}$-field formulation alone appears to result in computational difficulties in determining J^{ϕ} a better set of equations to begin with might then be the "hybrid" equations developed by Davis and Mittra [8]. In the latter a contribution from an $\underset{\sim}{H}$-field formulation is combined with an $\underset{\sim}{E}$-field formulation to result in a set of equations, in unknowns J^{ϕ} and J^{z}, which partially decouple. This is shown to permit a more accurate determination of J^{ϕ} for thin cylinders than does an $\underset{\sim}{E}$-field formulation alone.

3. Theoretical and Experimental Cavity Response Patterns

In Figure 3 a 4-inch diameter closed cylinder with a 1-inch diameter

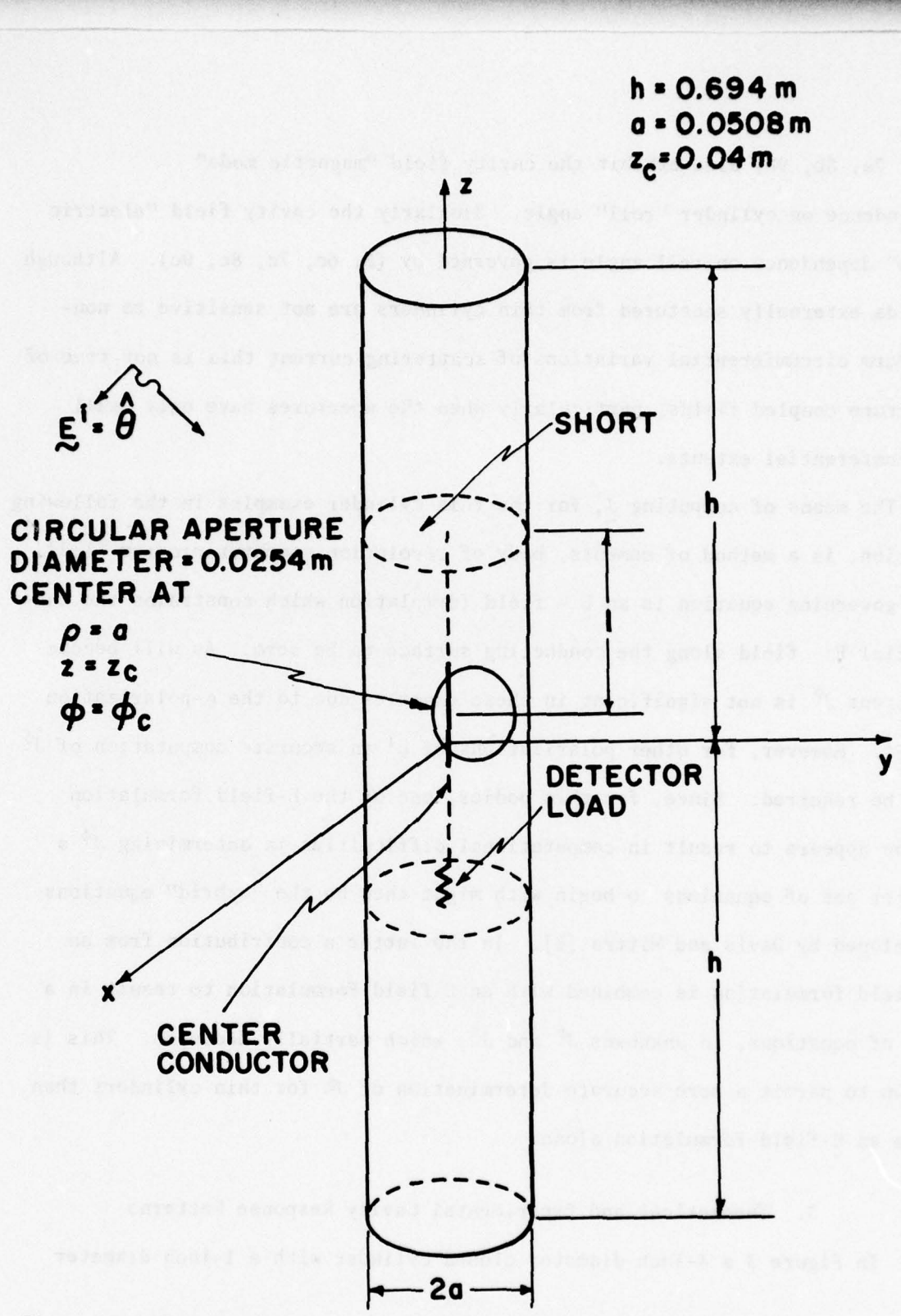

Figure 3. Characteristics of cylinder, sub-cavity and small circular aperture used in comparing theory with experiment.

circular aperture is shown. On the other side of the aperture is a thin-walled cylindrical cavity containing a thin axial conductor. This coaxial cavity is shorted at one end and loaded with a crystal detector at the other. In accordance with the discussion in the previous section the detected voltage, v, is given by (5) where $\underset{\sim}{P}$ is chosen to be the aperture center with coordinates $\rho=a$, $\phi=\phi_c$, $z=z_c$. In Figure 3 1 is the separation, parallel to the axis, between $\underset{\sim}{P}$ and the cavity short.

Experimental patterns of v, as $\underset{\sim}{E}^i$ varies with θ in the $\phi=0$ plane, have been taken at the Naval Surface Weapons Center (Dahlgren, Virginia) and repeated at the University of Colorado (Boulder, Colorado) [6]. According to (5) theoretical patterns formed from a linear combination of $\hat{J}^z$, $\hat{J}^\phi$, and $\nabla\cdot\hat{\underset{\sim}{J}}$ should agree with the experimental patterns of v. Theoretical values of $\hat{J}^z$, $\hat{J}^\phi$, and $\nabla\cdot\hat{\underset{\sim}{J}}$ were obtained with the body-of-revolution computer program. By treating A, A' , B as normalization constants a comparison between theoretical and experimental patterns of v is then possible. This comparison was performed and is described below for three cases: a) $l=0.5\lambda$ such that $B\simeq 0$ (magnetic mode), b) $l=0.25\lambda$ such that $A\simeq 0$ (electric mode), and c)$l=0.33\lambda$ (combined mode). In all cases the J^ϕ term was found insignificant and, hence, A' was set to zero.

3.1 Magnetic mode

At a frequency of 305 MHz the separation between aperture center and cavity short was adjusted such that $l=0.5\lambda$. From transmission line theory the cavity field was then expected to present an approximate null in $\underset{\sim}{E}$-field at the aperture. Since the $\nabla\cdot\hat{\underset{\sim}{J}}$ term in (5) is sensitive to the aperture-

normal component of $\underset{\sim}{E}$-field it thus was neglected. Also since $|\hat{J}^{\phi}|$ was found to be quite small (Figures 4 and 5) the $\hat{J}^{\phi}$ term in (5) was also neglected. The $|\hat{J}^{z}|$ shown in Figures 4 and 5 and the normalization $|A|$ =465 then resulted in a reasonable correspondence between theoretical and experimental patterns of v. This is shown in Figures 6 and 7. Figure 6 demonstrates a significant variation in current (~3dB peak-to-average ratio) in going from the illuminated side (ϕ_c=0) to the shadow side (ϕ_c=π) of the thin (a=0.05λ) cylindrical scatterer. It is the J_1^z and $-J_1^z$ terms in (6a) and (7a) respectively that govern this effect. Along the ϕ_c=$\pi/2$ and $3\pi/2$ paths J^z is given by (8a) and (9a). Here only the uniform current mode, J_o^z, is significant. Thus the variation between the ϕ_c= $\pi/2$ and $3\pi/2$ patterns (Figure 7) is theoretically zero and experimentally quite small.

3.2 Electric Mode

At a frequency of 200 MHz 1 was adjusted to l=0.25λ. This was expected to approximately null the cavity $\underset{\sim}{H}$-field at the aperture. Thus the $\hat{J}^z$ and $\hat{J}^{\phi}$ terms in (5) were omitted ($|\hat{J}^{\phi}|$ is again quite small as is evident from Figures 8 and 9). With $\nabla\hat{\cdot}\underset{\sim}{J}$ as shown in Figures 10 and 11 a normalization of $|B|$= 66.5 was then found to give good correspondence between theory and experiment for ϕ_c=0,π patterns of v. This is shown in Figure 12. The circumferential variation of v (peak-to-average ratio) is again about 3 dB which is especially significant since the cylinder radius is now only a=0.033λ. This front-to-back variation is due essentially to the $\dot{J}_1^z$ and $-\dot{J}_1^z$ terms in (6_c) and (7c) respectively. (As made evident in Figures 10

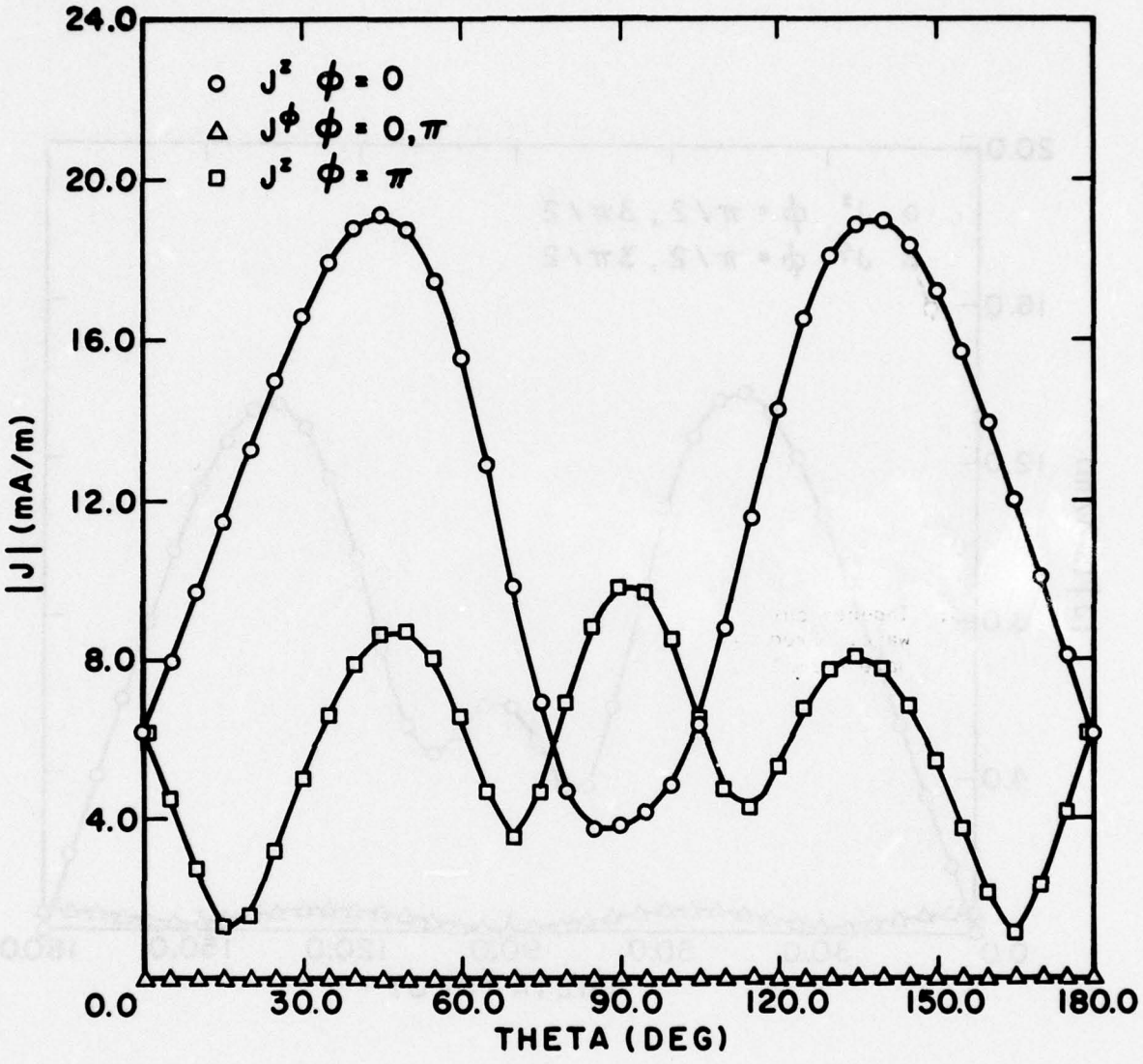

Figure 4. Induced current at aperture (shorted) vs. θ direction of incident wave. Freq. = 305 MHz. Aperture on illuminated side (∅=0) and then on shadow side (∅=π). $\underset{\sim}{E}^i$ = θV/m.

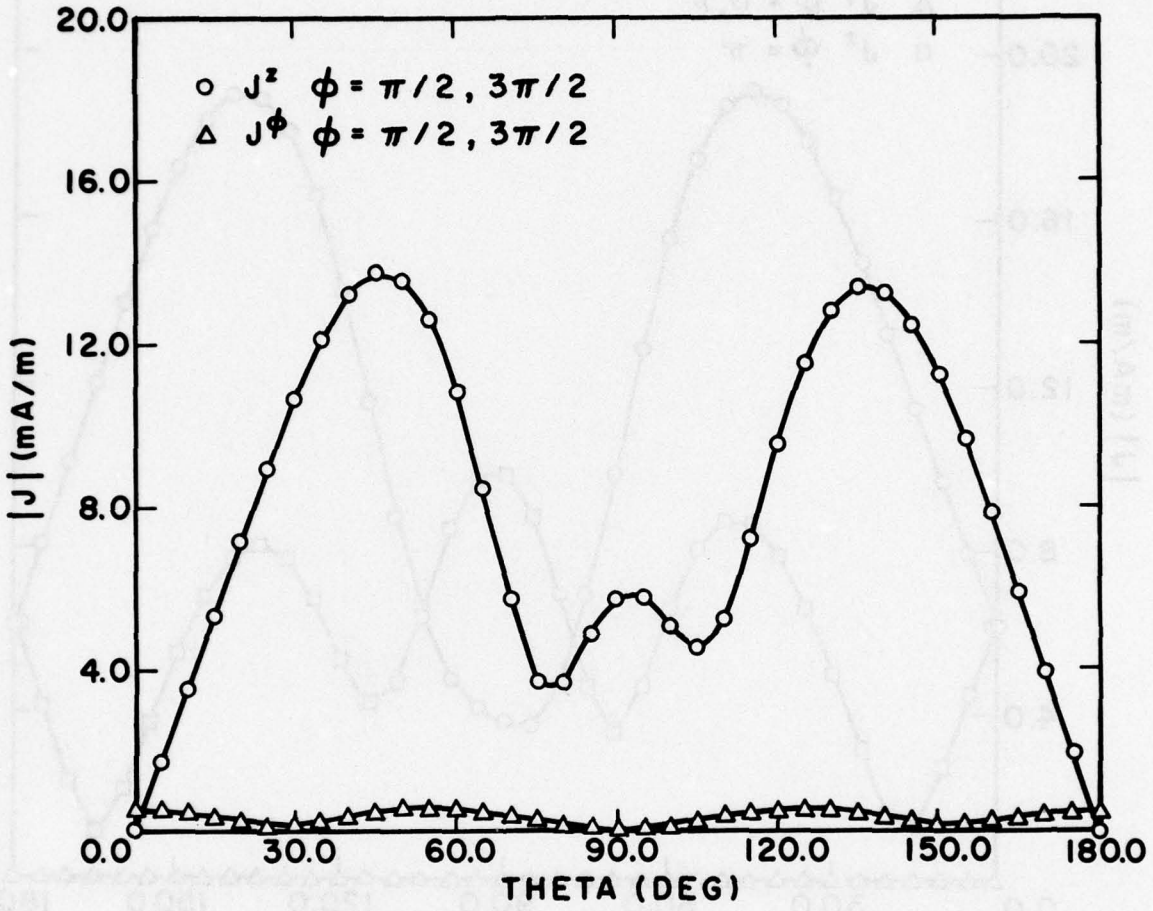

Figure 5. Induced current at aperture (shorted) vs. θ direction of incident wave. Freq. = 305 MHz. Aperture normal orthogonal to incident wave normal ($\emptyset=\pi/2$ and $3\pi/2$ roll angles). $\underset{\sim}{E}^i=\hat{\theta}$V/m.

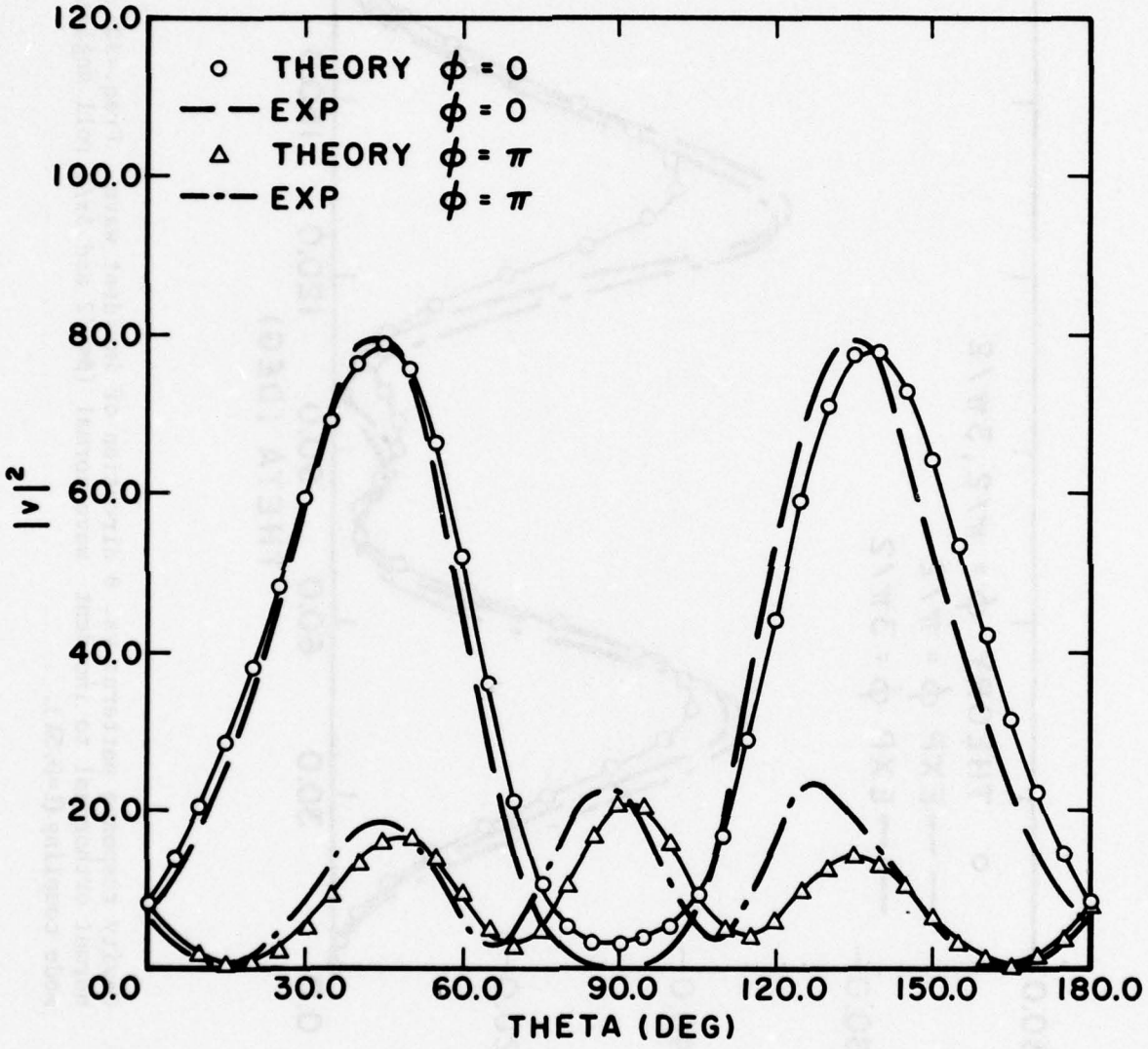

Figure 6. Cavity response patterns vs. θ direction of incident wave. Freq. =305 MHz. Aperture on illuminated side (Ø=0) and then on shadow side (Ø=π). Magnetic mode coupling (1=0.5λ).

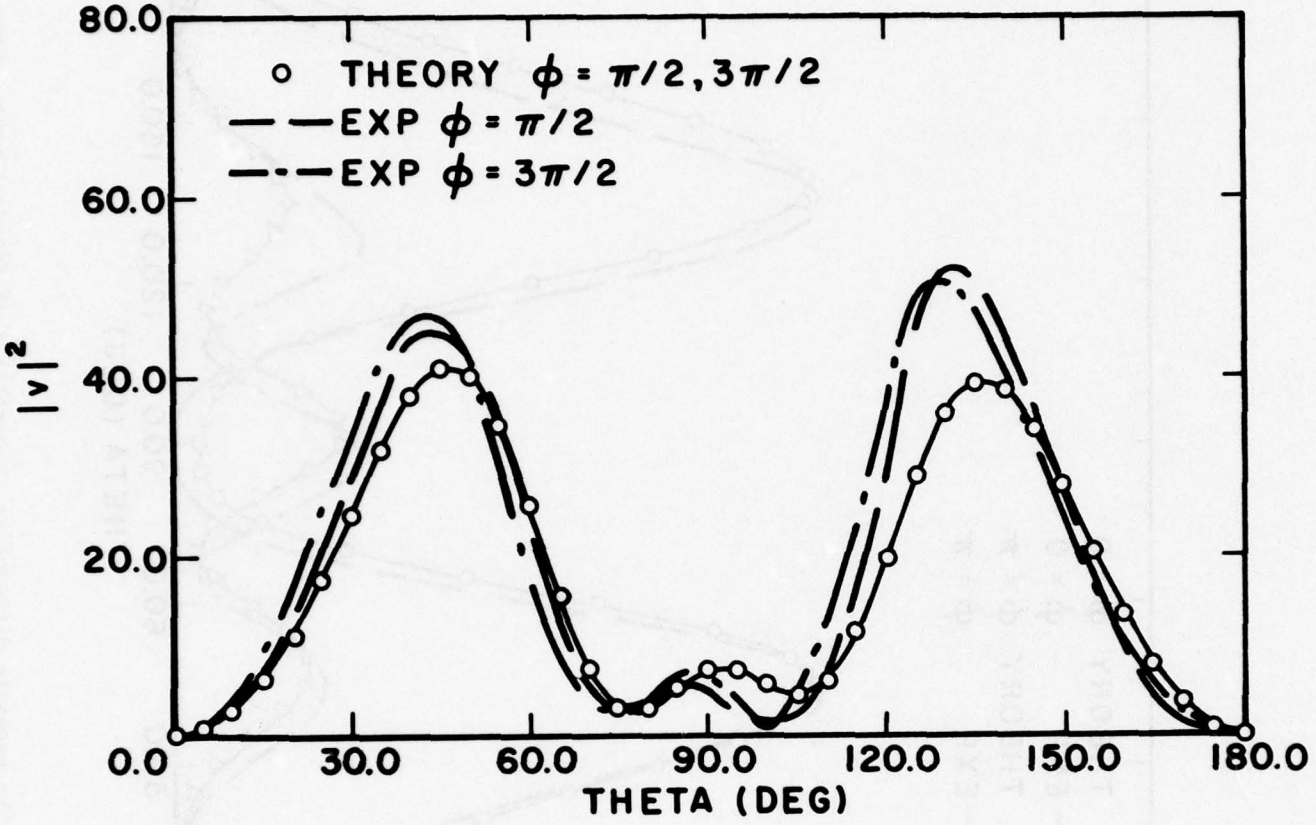

Figure 7. Cavity response patterns vs. θ direction of incident wave. Freq.=305 MHz. Aperture normal orthogonal to incident wave normal ($\emptyset=\pi/2$ and $3\pi/2$ roll angles). Magnetic mode coupling ($l=0.5\lambda$).

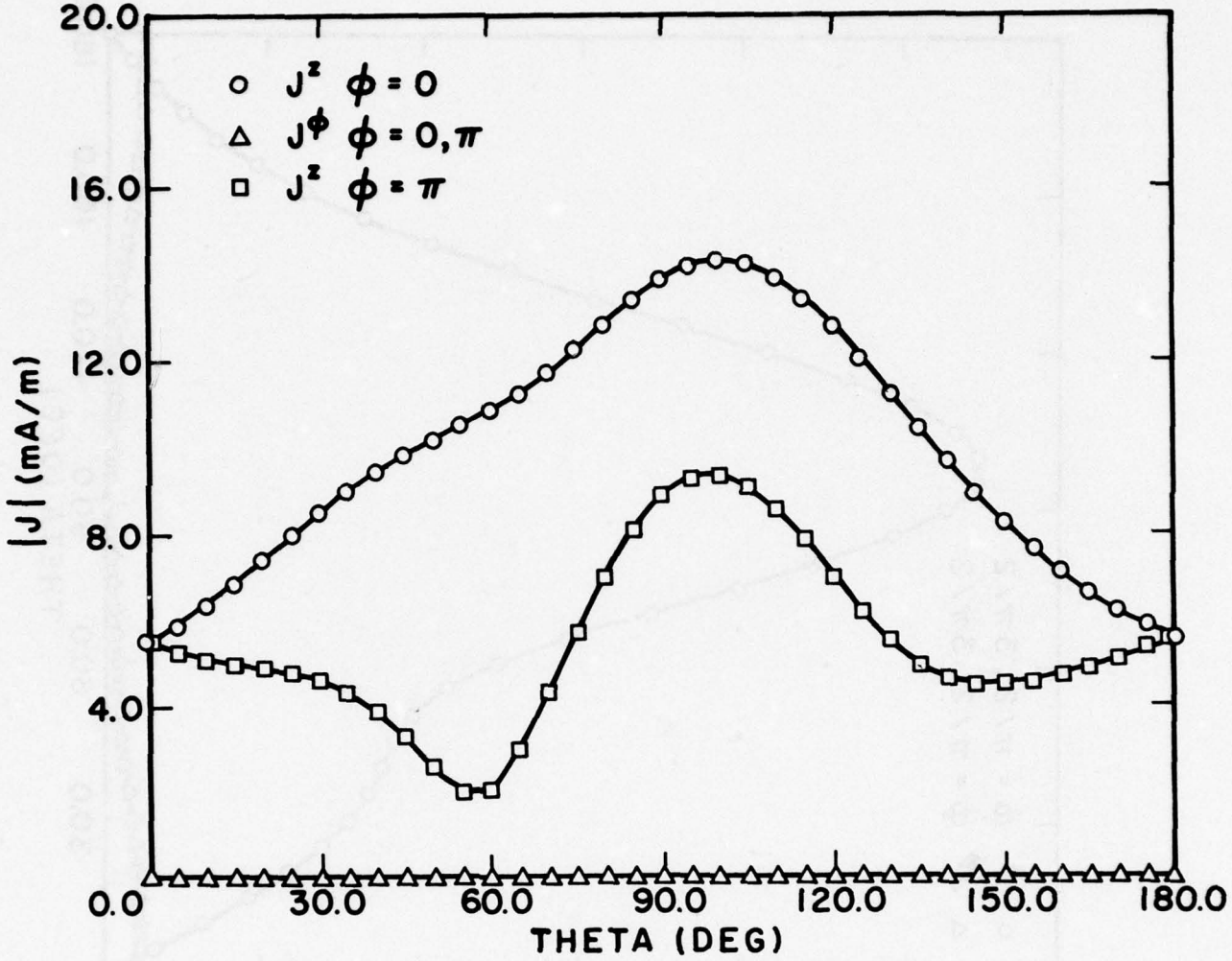

Figure 8. Same as for Figure 4 except now frequency = 200 MHz.

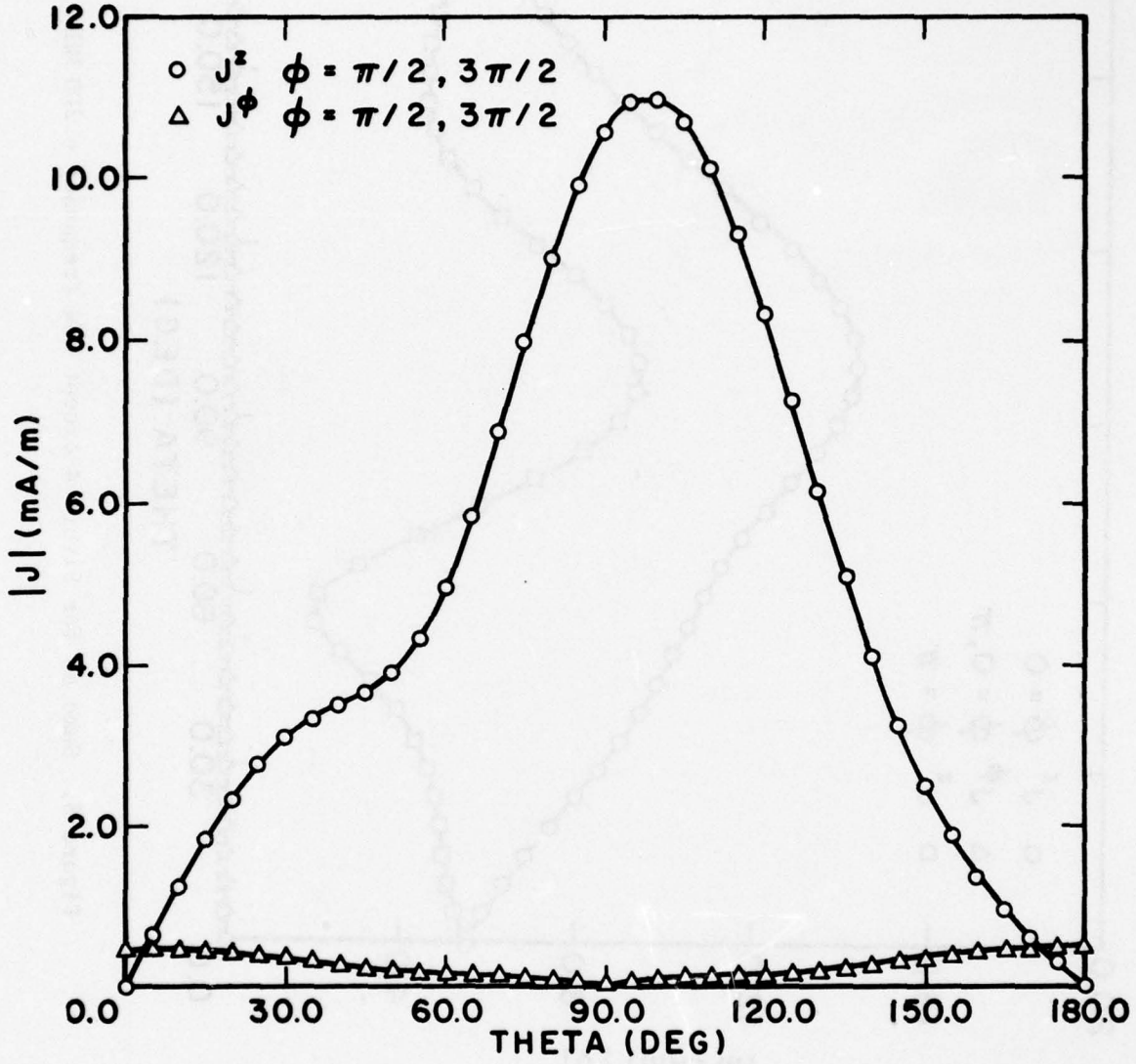

Figure 9. Same as for Figure 5 except now frequency = 200 MHz.

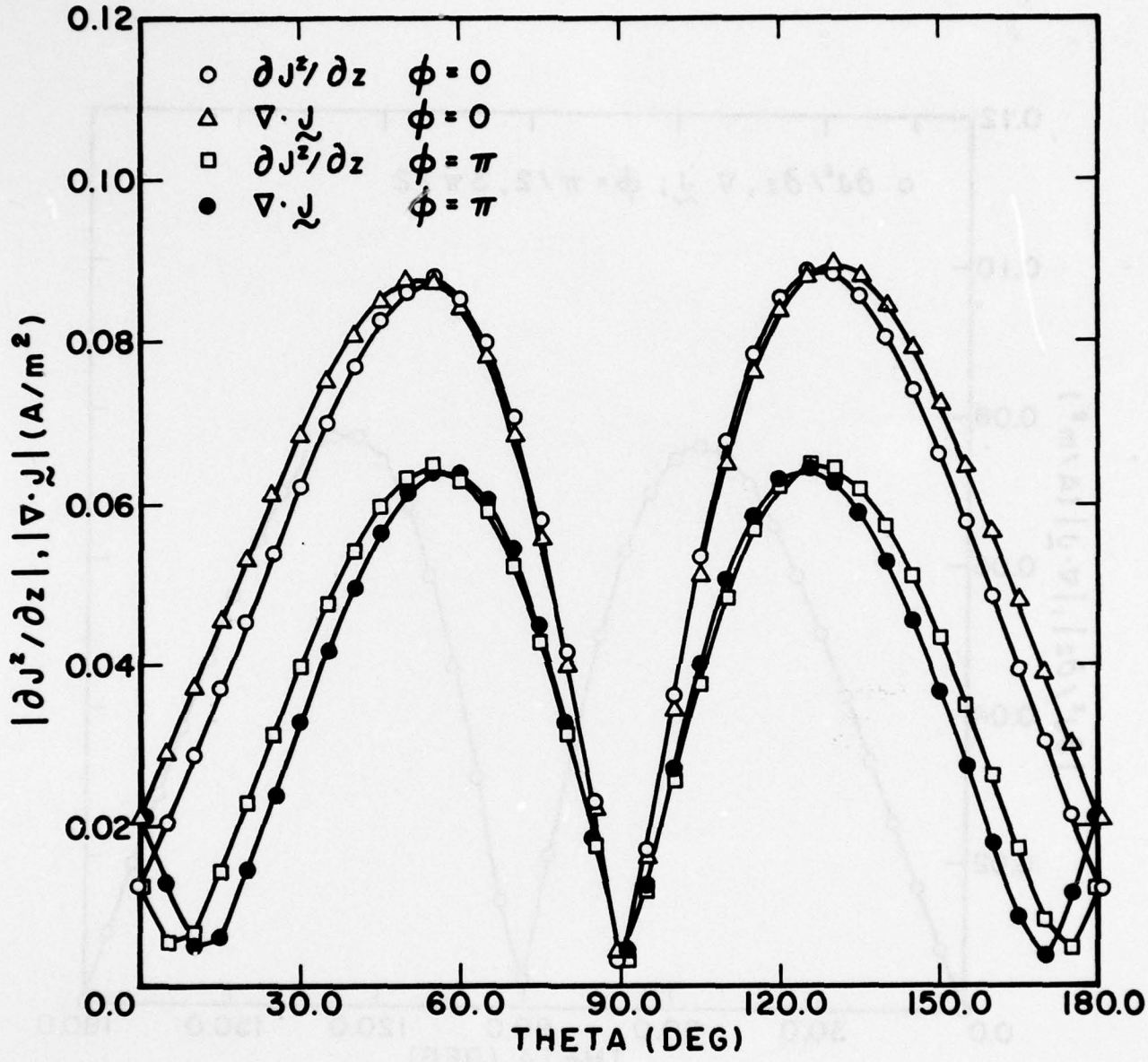

Figure 10. z-directed partial derivative and divergence of induced current at aperture (shorted) vs. θ direction of incident wave. Freq. = 200 MHz. Aperture on illuminated side (ϕ=0) and then on shadow side (ϕ=π). $\underset{\sim}{E}^i = \hat{\theta}$V/m.

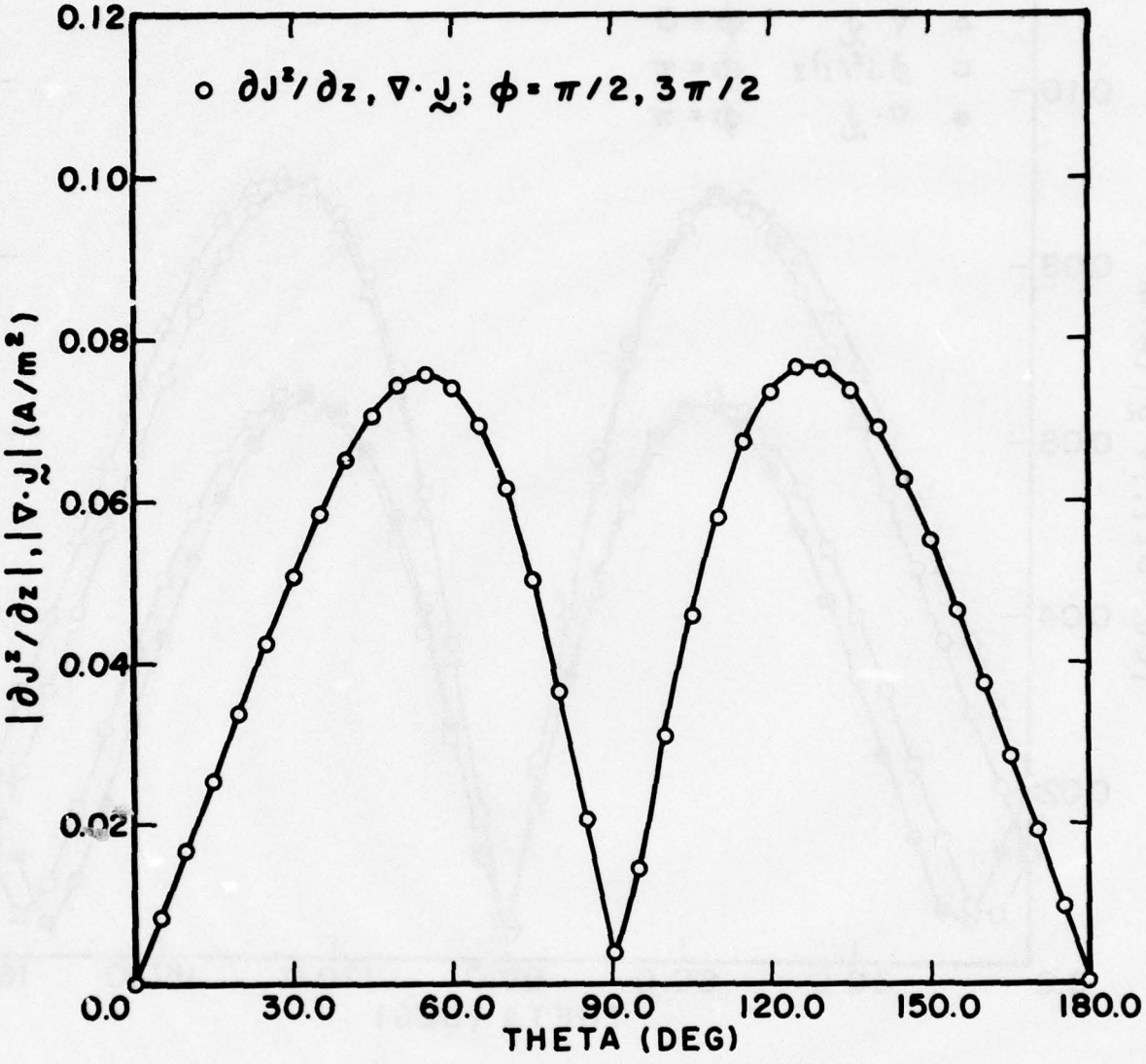

Figure 11. z-directed partial derivative and divergence of induced current at aperture (shorted) vs. θ direction of incident wave. Freq. = 200 MHz. Aperture normal orthogonal to incident wave normal (Ø=π/2 and 3π/2 roll angles). $\underset{\sim}{E}^i = \hat{\theta}$V/m.

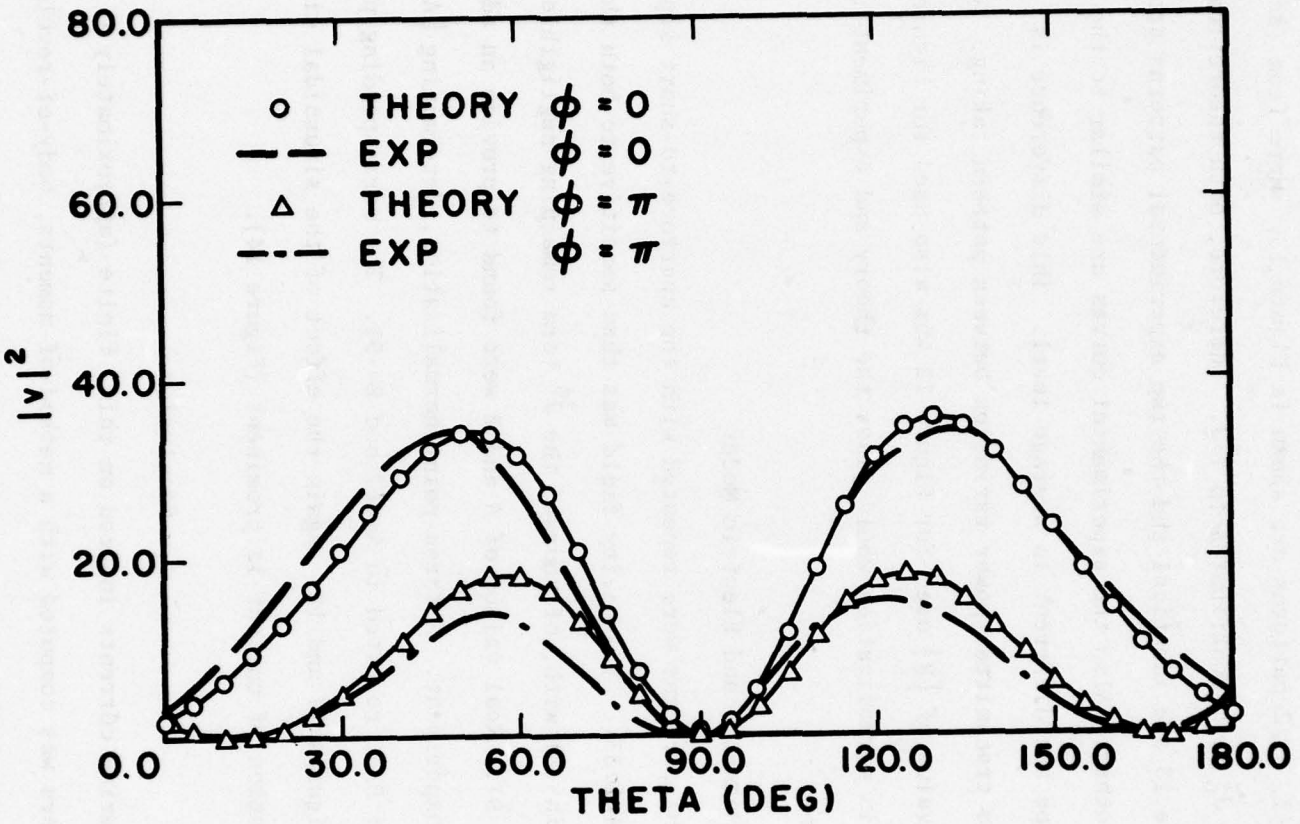

Figure 12 Cavity response patterns vs. θ direction of incident wave. Freq. = 200 MHz. Aperture on illuminated side (ϕ=0) and then on shadow side (ϕ=π). Electric mode coupling (l=0.25λ).

and 11, the $\pm J_1^{\phi}/a$ contributions to $\nabla \cdot \underset{\sim}{J}$ are small).

The $\phi_c = \pi/2, 3\pi/2$ patterns are shown in Figure 13. Here from (8c) and (9c), only the $\dot{J}_o^z$ term contributes to $\nabla \cdot \hat{\underset{\sim}{J}}$. Therefore, both theoretical patterns in Figure 13 are identical and the two experimental patterns are quite close to each other. Also the experimental curves are similar to the theoretical in shape but different in average level. This difference is probably due to transmitter power variation between pattern taking. Note that the same value of $|B|$ used for Figure 12 was also used for Figure 13. An adjustment in normalization would place the theory and experiment in better agreement.

3.3 Combined Magnetic and Electric Modes

The 200 MHz patterns were repeated with the aperture-to-short separation lengthened to $l=0.33\lambda$. The cavity field was then sensitive to both the $\hat{J}^z$ and $\nabla \cdot \hat{\underset{\sim}{J}}$ terms in (5) with, of course, the $\hat{J}^{\phi}$ term remaining negligible (Figures 8 and 9). Real values of A and B were found to provide an adequate fit of (5) to experiment. A three-point normalization, determining $|A|$, $|B|$ and the sign of B/A, resulted in A=467 and B=-91. The corresponding patterns are given in Figures 14 and 15. Again the effect of the sinusoidal circumferential variation of current is prominent (Figure 14).

4. Conclusion

The scattering currents induced on thin, finite (approximately λ in length) cylinders was computed with a method-of-moments, body-of-revolution computer program. Particular attention was paid to determining the circum-

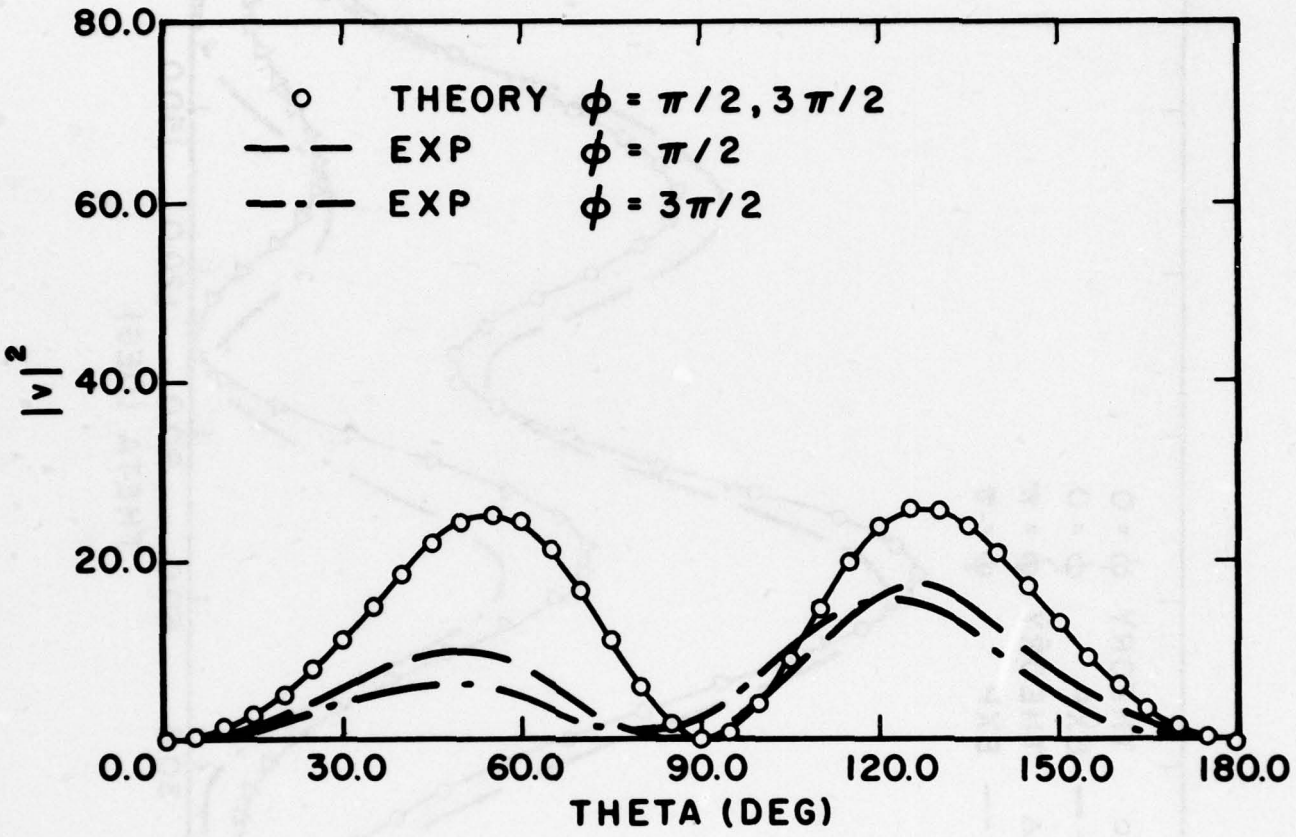

Figure 13. Cavity response patterns vs. θ direction of incident wave. Freq. = 200 MHz. Aperture normal orthogonal to incident wave normal (Ø=π/2 and 3π/2 roll angles). Electric mode coupling (1=0.25λ).

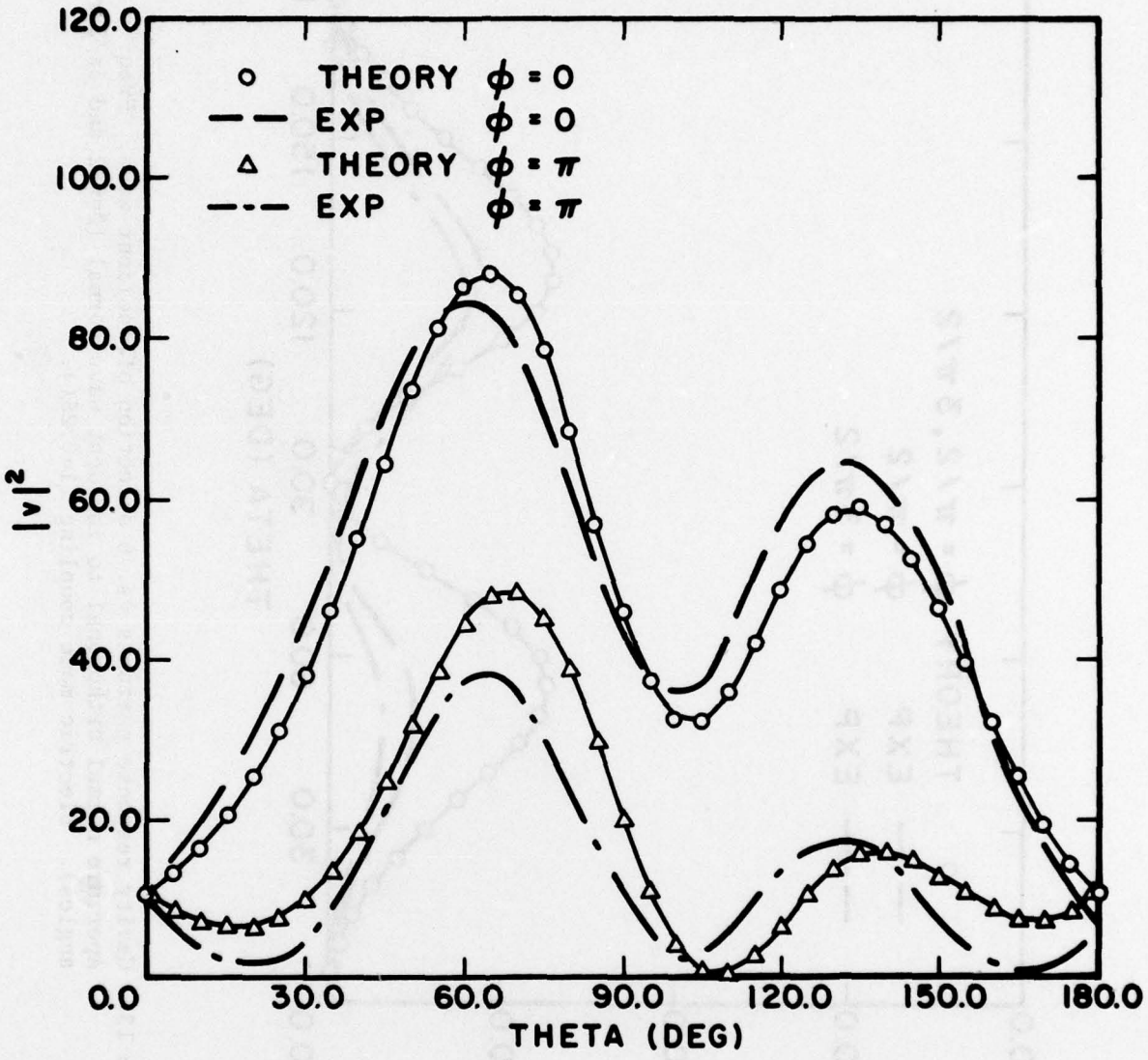

Figure 14. Same as for Figure 12 except now both electric and magnetic mode coupling significant (l=0.33λ).

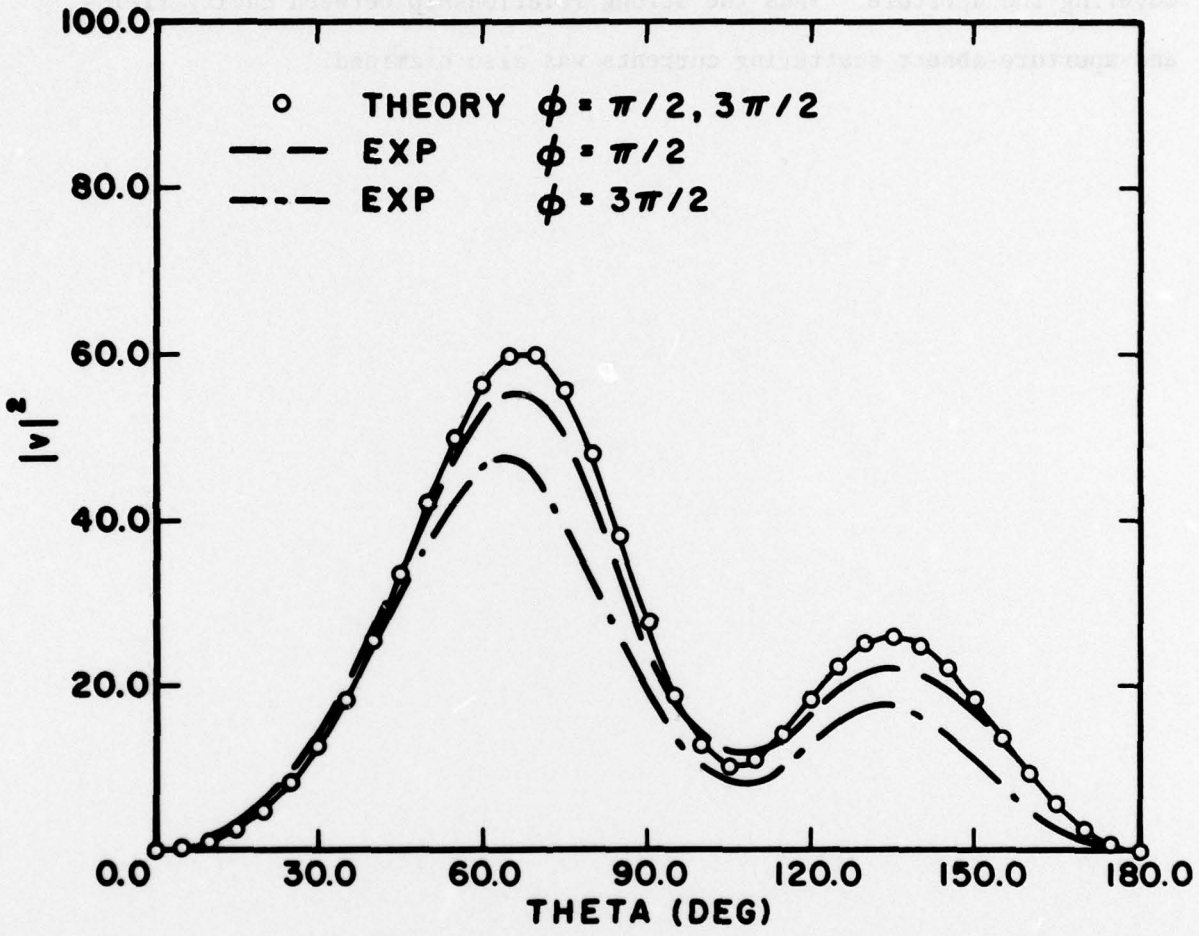

Figure 15. Same as for Figure 13 except now both electric and magnetic mode coupling significant (l=0.33λ).

ferential variation. This variation was found to be on the order of 3dB in peak-to-average value for cylinders with diameters of 0.1λ and 0.067λ. The accuracy of the computational method was verified by comparison with experiment after noting a relationship between the field coupled through a small aperture and the scattering current induced on a perfect conductor covering the aperture. Thus the strong relationship between cavity fields and aperture-absent scattering currents was also examined.

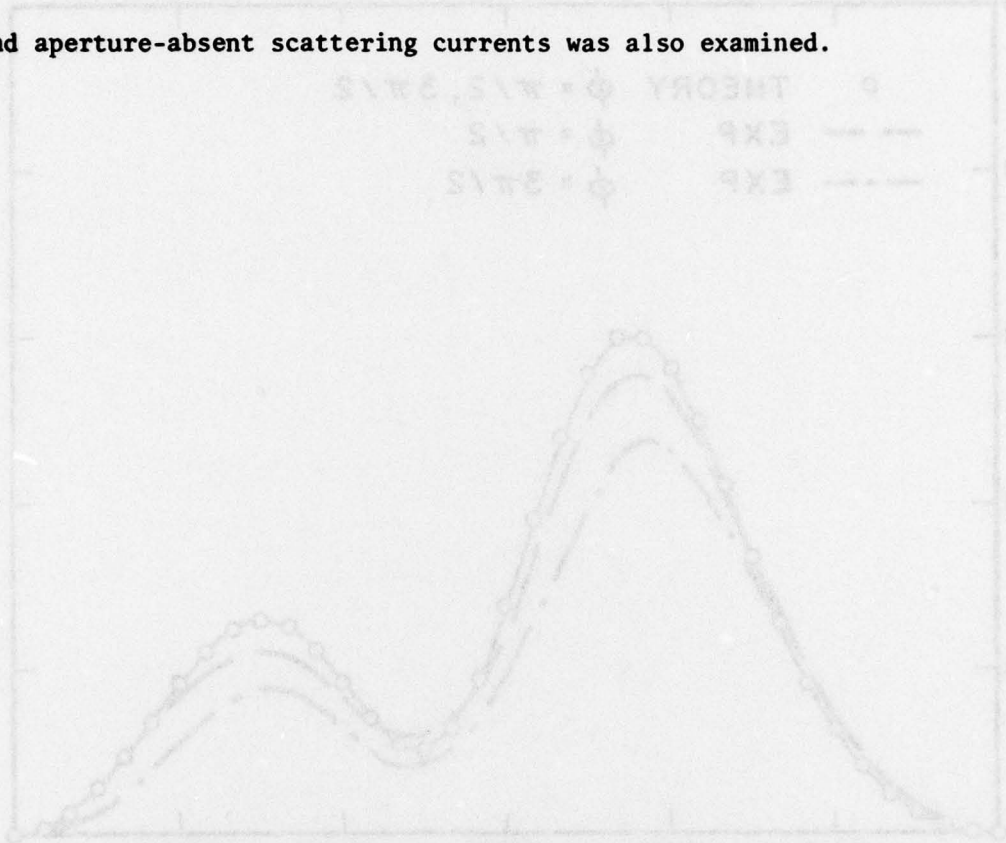

APPENDIX

Small-Hole Theory

The following development of "Bethe" Small-Hole theory [3,4] parallels that presented by Collin [5]. Whereas Collin began his development by deriving an equivalent magnetic current with which to excite a small aperture, the development here begins with an equivalent electric current aperture excitation. It is shown that this equivalent excitation can be approximated by a linear combination of the components of $\underset{\sim}{J}$ and the surface divergence of $\underset{\sim}{J}$ (charge) evaluated at a point within the aperture. Here $\underset{\sim}{J}$ is the aperture-shorted surface current induced on the external cavity surface. The only requirement is that the aperture plane be small and flat. The shape of the remaining cavity wall, even near the aperture, is arbitrary and conductors of any shape and number can reside anywhere within the cavity.

The development begins with an equivalence theorem, due to Schelkunoff [7], which represents the general aperture coupling problem by the superposition of a scattering problem and an aperture radiation problem. The former provides the source for the latter.

Figure A-1 (a) depicts a cavity of perfectly conducting wall except for an aperture of arbitrary size and shape. The sources are external to the cavity. The $\underset{\sim}{H}$-field at the aperture satisfies

$$\hat{n} \times (\underset{\sim}{H}_2 - \underset{\sim}{H}_1) = 0 \qquad \text{(A-1)}$$

where $\hat{n}$ is an inwardly directed unit vector normal to the cavity surface. If a perfect conductor is placed across the aperture, as shown in Figure

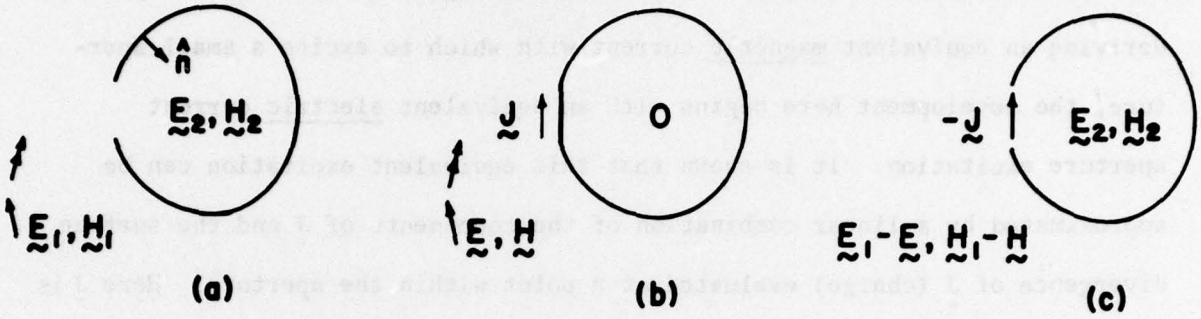

Figure A-1. Illustration of equivalence.

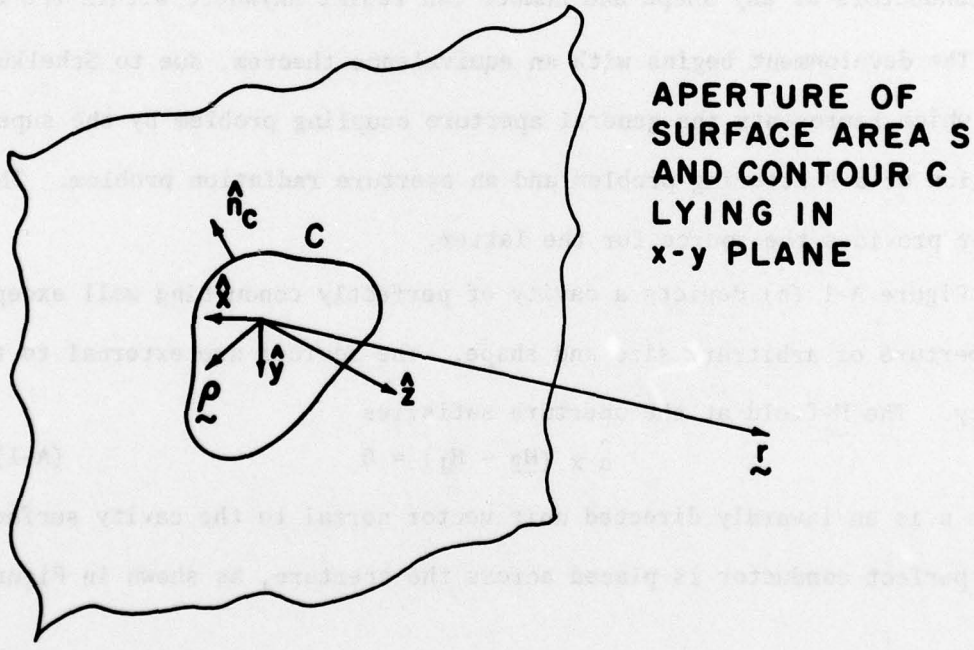

Figure A-2. Electrically small aperture observed from within a cavity.

A-1(b), the $\underset{\sim}{H}$-field discontinuity at the aperture must be supported by a current $\underset{\sim}{J}$ given by

$$-\hat{n} \times \underset{\sim}{H} = \underset{\sim}{J} \qquad \text{(A-2)}$$

The subtraction of fields in (b) from those in (a) results in the problem shown in Figure A-1(c). Here, the original sources are absent since, in their vicinity, the discontinuous fields that support them are the same as for (a) and (b). Also the $-\underset{\sim}{J}$ current source appearing in the aperture is required to support the $\underset{\sim}{H}$-field discontinuity determined by subtracting (A-2) from (A-1). The supperposition of (b) and (c) is equivalent to (a).

Since (b) is a straight-forward scattering problem the following development begins with (c) where the equivalent aperture current excitation, -J, is assumed known. By expanding $\underset{\sim}{J}$ in a Taylor Series it will be shown that for a sufficiently small, flat aperture, in an otherwise arbitrarily-shaped cavity, the internal field is excited by a linear combination of $\nabla \cdot \underset{\sim}{J}$ and the components of $\underset{\sim}{J}$. Of course, this excitation is identical to a linear combination of the normal electric and components of tangential magnetic fields on the external surface of the shorted aperture.

In Figure A-2 an electrically small, flat aperture opening into a cavity is shown as viewed from within the cavity. A coordinate system is chosen with z=0 plane parallel to the aperture surface S and origin within S. The unit vector, $\hat{n}_c$, lies in the z=0 plane and is normal to the aperture contour C. An aperture excitation, $-\underset{\sim}{J}$, is given which lies parallel to and within the aperture. With $\underset{\sim}{\rho}=x\hat{x}+y\hat{y}$ the first two terms of a Taylor Series expansion of each component of $\underset{\sim}{J}$ about the origin results in

$$\underset{\sim}{J}\ (\underset{\sim}{\rho}) \approx \underset{\sim}{J}\ (\underset{\sim}{0}) + x\frac{\partial \underset{\sim}{J}}{\partial x}\bigg|_{\underset{\sim}{\rho}=\underset{\sim}{0}} + y\frac{\partial \underset{\sim}{J}}{\partial y}\bigg|_{\underset{\sim}{\rho}=\underset{\sim}{0}}$$

$$\approx \underset{\sim}{J}\ (\underset{\sim}{0}) + (\underset{\sim}{\rho}\cdot\nabla\big|_{\underset{\sim}{\rho}=\underset{\sim}{0}})\ \underset{\sim}{J} \qquad \text{(A-3)}$$

The short-hand notation in (A-3) is obvious.

From reciprocity a field $\underset{\sim}{E}_2$ at point $\underset{\sim}{r}$ within the cavity is given by

$$\underset{\sim}{E}_2 \cdot \underset{\sim}{I1}^{r} = -\int_S \underset{\sim}{E}^{r} \cdot \underset{\sim}{J}\ ds \qquad \text{(A-4)}$$

where $\underset{\sim}{I1}^{r}$ is a current dipole located at $\underset{\sim}{r}$ and oriented parallel to a desired component of $\underset{\sim}{E}_2$, and $\underset{\sim}{E}^{r}$ is the field radiated by $\underset{\sim}{I1}^{r}$. Without loss of generality (A-4) may be written

$$\underset{\sim}{E}_2 \cdot \underset{\sim}{I1}^{r} = \int_S \underset{\sim}{M} \cdot \hat{z} \times \underset{\sim}{J}\ ds \qquad \text{(A-5)}$$

where the equivalent magnetic surface current $\underset{\sim}{M} = -\hat{z} \times \underset{\sim}{E}^{r}$ is defined. Note that $\underset{\sim}{M}$ can be thought of as a source lying just within the cavity and adjacent to the aperture after shorting. Then, in the absence of internal resonances, $\underset{\sim}{M}$ radiates, with $\underset{\sim}{I1}^{r}$ the same cavity field as occurs with $\underset{\sim}{I1}^{r}$ radiating alone and the aperture open.

The $\hat{z} \times \underset{\sim}{J}$ term in (A-5) can be approximated via (A-3) as

$$\hat{z} \times \underset{\sim}{J} \approx \hat{z} \times \underset{\sim}{J}\ (\underset{\sim}{0}) + (\underset{\sim}{\rho} \cdot \nabla\big|_{\underset{\sim}{\rho}=\underset{\sim}{0}})\ \hat{z} \times \underset{\sim}{J} \qquad \text{(A-6)}$$

By adding and subtracting an appropriate term (A-6) becomes

$$\hat{z} \times \underset{\sim}{J} \simeq \hat{z} \times \underset{\sim}{J}(Q) - 1/2\ (\nabla \cdot \underset{\sim}{J})\Big|_{\underset{\sim}{\rho}=Q} \underset{\sim}{\rho} \times \hat{z} + \underset{\sim}{H}' \tag{A-7}$$

where

$$\underset{\sim}{H}' = (\underset{\sim}{\rho} \cdot \nabla\Big|_{\underset{\sim}{\rho}=\underset{\sim}{0}})\ \hat{z} \times \underset{\sim}{J} + 1/2\ (\nabla \cdot \underset{\sim}{J})\Big|_{\underset{\sim}{\rho}=\underset{\sim}{0}} \underset{\sim}{\rho} \times \hat{z} \tag{A-8}$$

With the definition

$$\underset{\sim}{H}^t = \hat{z} \times \underset{\sim}{J} = H_x^t \hat{x} + H_y^t \hat{y}$$

(Note that $\underset{\sim}{H}^t$ is the tangential component of $\underset{\sim}{H}$-field external and adjacent to the shorted aperture.) it follows that

$$\underset{\sim}{H}' = x \left.\frac{\partial H_x^t}{\partial x}\right|_{\underset{\sim}{\rho}=\underset{\sim}{0}} \hat{x} + y \left.\frac{\partial H_y^t}{\partial y}\right|_{\underset{\sim}{\rho}=\underset{\sim}{0}} \hat{y}$$

$$+ 1/2\ (x\hat{y} + y\hat{x}) \left.\frac{\partial H_y^t}{\partial x}\right|_{\underset{\sim}{\rho}=\underset{\sim}{0}} + 1/2(x\hat{y} + y\hat{x}) \left.\frac{\partial H_x^t}{\partial y}\right|_{\underset{\sim}{\rho}=\underset{\sim}{0}} \tag{A-9}$$

The substitution of (A-7) into (A-5) gives

$$\underset{\sim}{E}_2 \cdot \underset{\sim}{I}_1 \simeq \hat{z} \times \underset{\sim}{J}(\underset{\sim}{0}) \cdot \int_S \underset{\sim}{M} ds + (\nabla \cdot \underset{\sim}{J})\Big|_{\underset{\sim}{\rho}=\underset{\sim}{0}} \hat{z} \cdot \int_S \frac{\underset{\sim}{\rho} \times \underset{\sim}{M} ds}{2}$$

$$+ \int_S \underset{\sim}{H}' \cdot \underset{\sim}{M}\ ds \tag{A-10}$$

The first integral in (A-10) is proportional to a magnetic dipole moment. To see this consider the integral

$$\int_S \nabla \cdot \phi \underset{\sim}{M}\, ds = \int_S (\phi \nabla \cdot \underset{\sim}{M} + \underset{\sim}{M} \cdot \nabla \phi)\, ds$$

$$= \oint_C \phi\, \underset{\sim}{M} \cdot \hat{n}_c dl$$

$$= \oint_C \phi\, \underset{\sim}{E}^r \cdot \hat{z} \times \hat{n}_c dl$$

$$= 0 \qquad \text{(A-11)}$$

where ϕ is an arbitrary scalar variable and one notes that $\underset{\sim}{E}^r \cdot \hat{z} \times \hat{n}_c = 0$ along C. Let $\phi = x$ in (A-11). Then

$$\int_S \underset{\sim}{M} \cdot \hat{x} ds = - \int_S x \nabla \cdot \underset{\sim}{M}\, ds$$

By multiplying the above by $\hat{x}$ and adding the result to a corresponding equation determined by setting $\phi = y$ in (A-11) one arrives at

$$\int_S \underset{\sim}{M}\, ds = - \int_S \underset{\sim}{\rho} \nabla \cdot \underset{\sim}{M}\, ds \qquad \text{(A-12)}$$

The integrals in (A-12) are proportional to the magnetic dipole moment

$$\underset{\sim}{m} = \frac{-1}{j\omega\mu_o} \int_S \underset{\sim}{\rho} \nabla \cdot \underset{\sim}{M}\, ds \qquad \text{(A-13)}$$

The second integral in (A-10) is proportional to the electric dipole moment

$$\underset{\sim}{p} = - \varepsilon_o \int_S \frac{\underset{\sim}{\rho} \times \underset{\sim}{M}}{2}\, ds \qquad \text{(A-14)}$$

The third integral in (A-10) after substitution from (A-9) is

$$\int_S \underset{\sim}{H'} \cdot \underset{\sim}{M} ds = \left.\frac{\partial H_x^t}{\partial x}\right|_{\underset{\sim}{\rho}=\underset{\sim}{0}} \int_S x M_x ds + \left.\frac{\partial H_y^t}{\partial y}\right|_{\underset{\sim}{\rho}=\underset{\sim}{0}} \int_S y\, M_y ds$$

$$+ \frac{1}{2} \left.\frac{\partial H_y^t}{\partial x}\right|_{\underset{\sim}{\rho}=\underset{\sim}{0}} \int_S (x M_y + y M_x) ds$$

$$+ \frac{1}{2} \left. \frac{\partial H_x^t}{\partial y} \right|_{\underset{\sim}{\rho}=\underset{\sim}{0}} \int_S (xM_y + yM_x)\, ds \qquad \text{(A-15)}$$

where $\underset{\sim}{M} = M_x \hat{x} + M_y \hat{y}$

Let ϕ in (A-11) be $\frac{x^2}{2}$, $\frac{y^2}{2}$ and xy in turn. Thus (A-15) becomes

$$-2\int_S \underset{\sim}{H}' \cdot \underset{\sim}{M} ds = \left. \frac{\partial H_x^t}{\partial x} \right|_{\underset{\sim}{\rho}=\underset{\sim}{0}} \int_S x^2 \nabla \cdot \underset{\sim}{M} ds + \left. \frac{\partial H_y^t}{\partial y} \right|_{\underset{\sim}{\rho}=\underset{\sim}{0}} \int_S y^2 \nabla \cdot \underset{\sim}{M} ds$$

$$+ \left. \frac{\partial H_y^t}{\partial x} \right|_{\underset{\sim}{\rho}=\underset{\sim}{0}} \int_S xy \nabla \cdot \underset{\sim}{M} ds + \left. \frac{\partial H_x^t}{\partial y} \right|_{\underset{\sim}{\rho}=\underset{\sim}{0}} \int_S xy \nabla \cdot \underset{\sim}{M} ds \qquad \text{(A-16)}$$

If one defines the dyadic magnetic quadrupole $\bar{q}$ by

$$\bar{q} = \hat{x}\hat{x} q_{xx} + \hat{y}\hat{y} q_{yy} + \hat{x}\hat{y} q_{xy} + \hat{y}\hat{x} q_{yx}$$

where

$$q_{xx} = \frac{-1}{j\omega\mu_o} \int_S x^2 \, \nabla \cdot \underset{\sim}{M} ds$$

$$q_{yy} = \frac{-1}{j\omega\mu_o} \int_S y^2 \, \nabla \cdot \underset{\sim}{M} ds$$

$$q_{xy} = q_{yx} = \frac{-1}{j\omega\mu_o} \int_S xy \nabla \cdot \underset{\sim}{M} ds$$

and notes the dyadic representation of $\nabla \underset{\sim}{H}^t$,

$$\nabla \underset{\sim}{H}^t = \hat{x}\hat{x} \frac{H_x^t}{\partial x} + \hat{y}\hat{y} \frac{\partial H_y^t}{\partial y} + \hat{x}\hat{y} \frac{\partial H_y^t}{\partial x} + \hat{y}\hat{x} \frac{\partial H_x^t}{\partial y}$$

then a concise form for (A-16) employs a "dyadic double-dot product" notation resulting in

$$\int_S \underset{\sim}{H}' \cdot \underset{\sim}{M} ds = \frac{j\omega\mu_o}{2} \left. \nabla \underset{\sim}{H}^t \right|_{\underset{\sim}{\rho}=\underset{\sim}{0}} : \bar{q} \qquad \text{(A-17)}$$

Equations (A-12, A-13, A-14, and A-17) in combination with (A-10) results in

$$\underset{\sim}{E}_2 \cdot \underset{\sim}{I}\underset{\sim}{1} \approx j\omega\mu_o \hat{z}x\underset{\sim}{J}(\underset{\sim}{Q}) \cdot \underset{\sim}{m} - \frac{1}{\epsilon_o} (\nabla\cdot\underset{\sim}{J})\Big|_{\underset{\sim}{\rho}=\underset{\sim}{Q}} \hat{z}\cdot\underset{\sim}{p} + \frac{j\omega\mu_o}{2} \nabla\underset{\sim}{H}^t\Big|_{\underset{\sim}{\rho}=0} : \overline{q} \qquad \text{(A-18)}$$

The quadrapole term in (A-18) depends on the square of the aperture dimension and, hence, can be neglected for a sufficiently small aperture. Thus,

$$\underset{\sim}{E}_2 \cdot \underset{\sim}{I}\underset{\sim}{1} \approx j\omega\mu_o \hat{z}x\underset{\sim}{J}(\underset{\sim}{Q}) \cdot \underset{\sim}{m} - \frac{1}{\epsilon_o} \nabla\cdot\underset{\sim}{J}\Big|_{\underset{\sim}{\rho}=0} \hat{z}\cdot\underset{\sim}{p}$$

as was to be shown.

REFERENCES

[1]. R.F. Harrington and J.R. Mautz, "Radiation and Scattering from Bodies of Revolution, " Final Report, prepared for Air Force Cambridge Research Laboratories, Bedford, Mass., under Contract No. F19628-67-C-0233, July 1969.

[2]. J.R. Mautz and R.F. Harrington, "Generalized Network Parameters for Bodies of Revolution," Scientific Report No. 1, Contract No. F-19628-67-C-0233, Air Force Cambridge Research Laboratories, Bedford, Mass., with Syracuse University, Syracuse, N.Y., May 1968. Or see instead: J.R. Mautz and R.F. Harrington, "Radiation and Scattering from Bodies of Revolution", Applied Scientific Research, Vol. 20, 1969.

[3]. H.A. Bethe, "Theory of Diffraction by Small Holes," Phys. Rev, vol.66, pp. 163-182, 1944.

[4]. C.J. Bouwkamp, "Diffraction Theory", Repts. Prog. in Phys., vol. 17, pp. 75-100, 1954.

[5]. R.E. Collin, Field Theory for Guided Waves, McGraw-Hill, pp. 285-302, 1960.

[6]. C.T. Johnk, et. al., "Electromagnetic Penetration into Cylindrical Enclosures", Sci. Rep. No. 17; Prepared for U.S. Naval Surface Weapons Center, Dahlgren, Virginia, by the Electromagnetics Laboratory, Dept. of Electrical Engineering, Univ. of Colorado, Boulder, Colorado under Contract no. N00173-74-C-0556, January 1976.

[7]. S.A. Schelkunoff, "Field Equivalence Theorems," Comm. on Pure and Applied Math., vol. 4, pp. 43-59, June 1951.

[8]. W.A. Davis and R. Mittra, "A New Approach to the thin Scatterer Problem Using Hybrid Equations", IEEE Trans. on Antennas and Propagation, vol. AP-25, pp. 402-406, May 1977.

[9]. M. I. Sancer, et. al., "Relationship Between Total Currents and Surface Current Densities Induced on Aircraft and Cylinders ", AFWL Interaction Note 194, Kirtland AFB, N.M., Aug. 1974.

[10]. C.D. Taylor and C. W. Harrison, "Current and Charge Densities Induced on the Surface of a Prolate Spheroid Illuminated by a Plane Wave Electromagnetic Field", IEEE Transactions on Electromagnetic Compatibility, vol. EMC - 19, pp. 127 - 131, Aug. 1977.

MISSION
of
Rome Air Development Center

RADC plans and conducts research, exploratory and advanced development programs in command, control, and communications (C^3) activities, and in the C^3 areas of information sciences and intelligence. The principal technical mission areas are communications, electromagnetic guidance and control, surveillance of ground and aerospace objects, intelligence data collection and handling, information system technology, ionospheric propagation, solid state sciences, microwave physics and electronic reliability, maintainability and compatibility.